Initial stages of InAs epitaxy on vicinal GaAs(001)-(2×4)

V. Bressler-Hill
Center for Quantized Electronic Structures, University of California, Santa Barbara, California 93106 and Chemical Engineering Department, University of California, Santa Barbara, California 93106

A. Lorke*
Materials Department, University of California, Santa Barbara, California 93106

S. Varma
Chemical Engineering Department, University of California, Santa Barbara, California 93106

P. M. Petroff and K. Pond
Center for Quantized Electronic Structures, University of California, Santa Barbara, California 93106 and Materials Department, University of California, Santa Barbara, California 93106

W. H. Weinberg
Center for Quantized Electronic Structures, University of California, Santa Barbara, California 93106 and Chemical Engineering Department, University of California, Santa Barbara, California 93106
(Received 24 March 1994; revised manuscript received 9 May 1994)

Using an ultrahigh-vacuum scanning tunneling microscope, we have studied molecular-beam epitaxy-grown GaAs on vicinal (001)-(2×4) surfaces decorated at 450 °C with submonolayer coverages of InAs. On surfaces misoriented towards the [110] direction (*A* type), we have observed that the InAs nucleates in terrace defects, at the step edges, and on the terraces. Predominantly, we observe nucleation on the terraces with the formation of islands. The InAs islands are locally ordered into a (4×4) or a $c(4\times4)$ In-terminated reconstruction, which easily distinguishes them from the (2×4) GaAs substrate. The InAs growth is predominantly In-rich, although some islands exhibit domains of As-terminated $(2\times n)$ reconstruction. With increasing coverage, the anisotropy and density of the islands increases on the terraces while growth at the step edges remains almost constant. Furthermore, the size distribution of the islands in the [110] direction is narrow and independent of coverage for fractional coverages of InAs below $\theta=0.75$ ML, indicating that there is a preferred island *width*. On surfaces misoriented towards the $[\bar{1}10]$ direction (*B* type), InAs nucleates predominantly at step edges and in the terrace vacancies. Island growth is observed on terraces larger than 8 nm, with the anisotropy of the islands dependent on the corresponding terrace width. As for the *A*-type surface, the islands are found to have a preferred width in the [110] direction of 4±1 nm. We suggest that strain effects are limiting the island size in the [110] direction.

I. INTRODUCTION

Recently, it was demonstrated that deposition of modest amounts of InAs on GaAs results in the formation of coherently strained InAs clusters or elongated islands which exhibit unusual optical and transport properties.[1-3] These properties are thought to be the result of two- and three-dimensional carrier confinement in the InAs within the GaAs matrix. In addition, strained epitaxial layers or islands provide an additional parameter for the optimization of the optical properties of the heterostructures and quantum wells. Moreover, this is an excellent system for studying the effects of strain on the atomic structure (7% lattice mismatch) since the binding energy of the In with the GaAs substrate does not result in the exchange of the substrate Ga atoms with the newly adsorbed In atoms, and the interfacial energy is sufficiently small to allow two-dimensional growth at low coverage.

The initial stages of InAs molecular-beam epitaxial (MBE) growth on GaAs(001)-$c(4\times4)$ at 350°C was recently investigated using reflection anisotropy spectroscopy (RAS).[4] It was reported that the RAS signal underwent significant changes upon InAs adsorption for coverages as low as 0.17 ML (monolayer). At this coverage changes of the surface reconstruction are responsible for the signal variation. Thus, submonolayer InAs coverages induce significant changes in the long-range order of the surface. However, the nature of the *local* structural changes are difficult to determine using large-scale probes. Ploog and Brandt[5] monitored the MBE growth of InAs on GaAs(001)-$c(4\times4)$ at 420°C using reflection high-energy electron diffraction (RHEED) and observed that the $c(4\times4)$ superstructure changes to a (2×3) superstructure after deposition of 0.6 ML of InAs. From the characteristics of the RHEED pattern, they concluded that InAs growth at this temperature occurs mainly by step-edge nucleation.

Using an ultrahigh vacuum (UHV) scanning tunneling microscope (STM), we have studied MBE-grown GaAs on vicinal (001)-(2×4) surfaces with submonolayer coverages of InAs. We have investigated surfaces misoriented toward the [110] (*A*-type) and [$\bar{1}$10] directions (*B*-type), and we observe that the preferred InAs nucleation sites are different for the two orientations. In addition, regardless of coverage ($\theta < 0.75$ ML) or surface misorientation, InAs islands are observed which have a preferred width in the [110] direction. We suggest that strain effects are limiting the island size in the [110] direction.

This paper is organized as follows. In Sec. II we delineate the experimental procedures that, among other things, involve the quench and vacuum transfer of the MBE-grown samples from the MBE system into the UHV-STM chamber. High-resolution STM images of InAs on the A-type 1°-GaAs(001) surface as a function of coverage are presented in Secs. III A and III B. In Sec. III B a model for the local InAs structure is given, and a statistical comparison of the InAs islands is delineated. Section III C concerns the results of InAs deposition on the *B*-type 1°-GaAs(001) surface. In Sec. IV the factors that may be involved in producing the observed uniform island width in the [110] direction are discussed. Finally, our conclusions are presented in Sec. V.

II. EXPERIMENTAL PROCEDURES

The two vicinal samples which were investigated are misoriented by 1°±0.1° toward the [110] and [$\bar{1}$10] azimuths, respectively, and they are mechanically held with tantalum sample holders to provide compatibility to standard 3-in. MBE sample holders and to the STM. Holes have been cut into the MBE block and the tantalum holders to allow direct radiative heating of the samples by a filament placed behind the MBE sample holder. This configuration allows for compatibility between the MBE machine and the STM, but it has the disadvantage that some temperature uniformity is lost during the MBE growth. The temperature is monitored both by observation of the oxide desorption at 630°C and by direct measurements using a pyrometer. We estimate a ±10 °C error in our temperature calibration.

The growth begins with thermal desorption of the oxide under an As flux at a substrate temperature of 630 °C. A 500-nm GaAs buffer layer was grown at a substrate temperature of 600 °C, under an As beam flux of $P_{As} = 3 \times 10^{-6}$ Torr. Then, with the As shutter left open, a 120-nm thick tilted superlattice (TSL) was grown by depositing alternating layers of 0.5-ML GaAs and 0.5-ML AlAs under the same growth conditions as for the GaAs buffer layer.[6] The rates used for the Ga and Al deposition are 0.23 and 0.3 ML/s, respectively. A 4-ML cap of GaAs was then deposited to regain a stoichiometric GaAs(001)-(2×4) surface.[7] This growth sequence has proved to result in periodic step structures and well-ordered (2×4)-reconstructed terraces. The TSL layer was not grown on the *B*-type surfaces, since there is no evidence for step bunching on this surface.[8] The samples were Si doped ($N_d = 1 \times 10^{18}$ cm^{-3}). All samples were quenched to room temperature by decreasing both the substrate temperature and the As pressure. The RHEED pattern remained (2×4) at room temperature. A control sample was removed from the growth stage, and the remaining samples were returned to the growth chamber for InAs deposition. The samples were carefully heated to 450 °C under low As background pressure to maintain the (2×4) reconstruction, and various fractional coverages ($\theta = 0.15$, 0.35, and 0.75) of InAs were deposited. The In was deposited at a rate of 0.25 ML/s with the As shutter closed (as being supplied by its background partial pressure).[9] During InAs deposition the RHEED pattern in the [$\bar{1}$10] azimuth was monitored. The extent to which the RHEED pattern was altered depended on the amount of InAs deposited. In particular, at $\theta = 0.15$ ML the RHEED 4× pattern became diffuse; at $\theta = 0.35$ ML it became a diffuse 2×, and at $\theta = 0.75$ ML only the specular intensity remained. This quenching and deposition procedure results in the GaAs-related (2×4) reconstruction on both the reference sample and the clean areas of the InAs-deposited samples. All samples were then removed from the MBE system. An ion-pumped interlock shuttle was used to transfer the samples to the STM chamber under UHV conditions.[10] The transfer procedure was concluded in less than 1 h, and the pressure during transport was maintained below 1×10^{-9} Torr. The STM measurements were performed in an UHV chamber with a base pressure of 3×10^{-10} Torr. Platinum iridium tips were used which can be cleaned *in situ* by electron bombardment to give atomic resolution.[11] All STM images which are shown were measured at a tunneling current of 0.1 nA and a sample bias of −2.4 to −3.5 V. All together 15 samples from five growth runs were studied. For every coverage of InAs, a total area of 0.23 μm^2 was examined with STM.

III. RESULTS

A. InAs deposition on *A*-type surfaces: low coverage

Figure 1 shows a STM image of a clean 1° *A*-type GaAs(001)-(2×4) surface. The steps are regularly spaced, and the average terrace width on this surface was calculated to be 240 Å, indicating a local misorientation of 0.67°. The (2×4) reconstruction is also resolved in the image. For reference a (2×4) unit cell is outlined in the high-resolution image shown in Fig. 2. The (2×4) structure produced using our growth and quenching procedures consists predominantly of two arsenic dimers and two missing dimers. There are two structures that have been proposed for such a reconstruction,[12,13] which differ from one another in the composition of the second layer. In Chadi's model,[12] the second-layer two-fold-coordinated Ga is absent, and the third-layer As is dimerized. The model proposed by Farrell, Harbison, and Peterson,[13] on the other hand, has the second-layer threefold-coordinated Ga dimerized to the twofold-coordinated Ga. Either model could be correct since the nature of the atomic composition of the missing dimer area of the unit cell has not been determined experimentally.

A high-resolution STM image of the clean GaAs sur-

FIG. 1. A 200×200 nm^2 STM image of a clean 1° A-type GaAs(001)-(2×4) surface.

face after deposition of 0.15 ML of InAs is shown in Fig. 2. Since the coverage is low, the GaAs-related (2×4) reconstruction is still observed. In this high-resolution image, the two dimers in the (2×4) unit cell are clearly resolved, but small areas of the surface now appear different from the surrounding reconstruction. These

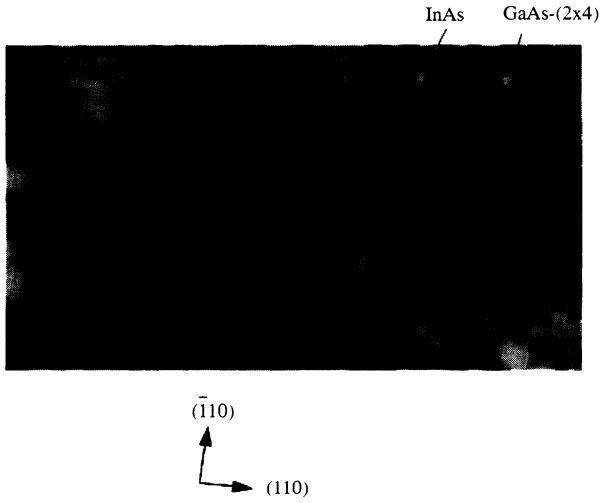

FIG. 2. A high-resolution STM image of the 1° A-type GaAs(001)-(2×4) surface after deposition of 0.15 ML of InAs. Note the clear resolution of the GaAs-related (2×4) unit cell. An InAs island is indicated with an arrow. The size of the image is 30×15 nm^2.

patches are about 1.5 Å above the GaAs surface, and are clearly not (2×4) reconstructed. We conclude that these patches or islands are composed of InAs, since the coverage of these islands determined from the STM images agrees with the deposited InAs coverage (calibrated using RHEED oscillations). The existence of islands shows that In is mobile on the surface at this deposition temperature (450 °C). Although a step edge is not shown in Fig. 2, we did not observe preferential growth at the step edges. In fact, we observed many step edges that have no obvious InAs growth. The InAs islands on the terrace are slightly elongated in the [1̄10] direction (as discussed below). Anisotropic islands elongated in the [1̄10] direction have also been observed after homeopitaxy of GaAs on the GaAs(001)-(2×4) surface.[14–18] In the latter case, the anisotropy in the island shape is thought to be due to the different reactivities of the step edges[19] and the lower diffusion barrier for Ga along the [1̄10] direction.[20] In the case of InAs on GaAs(001), strain-relief mechanisms in addition to diffusion and reaction anisotropies must be considered, as will be discussed in Sec. IV.

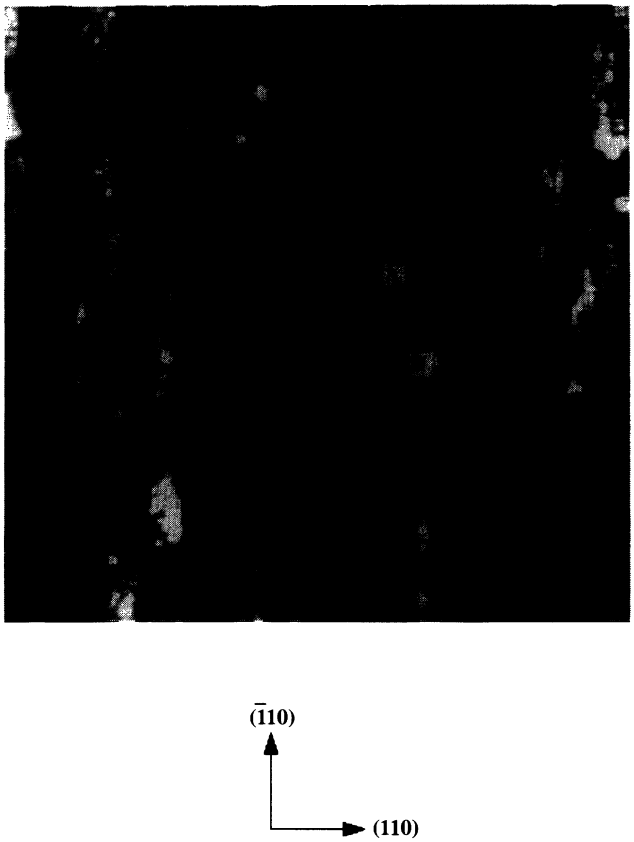

FIG. 3. A 100×100-nm^2 STM image of the 1° A-type GaAs(001)-(2×4) surface with an InAs coverage of θ=0.35. For clarification, the step edges have been outlined in black. Note the anisotropy of the InAs islands. Some islands exhibit separate domains of indium and arsenic termination. An In-terminated domain (A) and an As-terminated domain (B) are indicated with arrows. The areas that are highlighted with the dashed line are shown in Fig. 4.

B. InAs deposition on *A*-type surfaces: increased coverages

In Fig. 3 a high-resolution STM image of the GaAs surface after a deposition of 0.35 ML of InAs is shown. The step edges are uniformly spaced and have been outlined in black to clearly distinguish them from the terraces. The GaAs-(2×4) reconstruction is still observed, and the InAs is again distinguished from the surrounding GaAs-(2×4) by the different structure observed within the InAs patches. As observed for the lower coverage, InAs predominantly forms islands on the terrace. At this coverage the InAs-related structure is also observed on some of the step edges. The growth on the terraces, though, is 2.5 times more likely than at the step edge. Generally, only 1–2 nm of InAs growth at the step edge in the [110] direction is observed, and many areas of the step edge remain InAs free, indicating that the step edge is not the preferred nucleation site at this temperature. In addition, InAs is also observed in vacancies on the clean GaAs terrace (cf., Fig. 1). These vacancies are probably clusters of missing (2×4) GaAs unit cells. Indeed, few vacancies are found that have not been filled with InAs. Most of the patches of InAs, whether island, step, or defect related, are ordered. To emphasize this order, zoomed images of Fig. 3 (outlined with a dashed box) are shown in Fig. 4. Figure 4(a) shows the growth of an island from a step edge as well as other smaller islands not associated with a step. The alternating structure of the bright areas within the islands is clearly resolved. In Fig. 4(b) a high-resolution image of another island is shown which illustrates the alternating structure.

To determine the nature of the local structure of InAs, the images were calibrated in the [110] and [$\bar{1}$10] directions with the known periodicity of the (2×4) GaAs reconstruction as a standard. From a detailed line-scan analysis of the calibrated images, we have determined that the ordered bright areas in the islands are consistent with the size of two dimers oriented along the [110] direction. If a line scan is measured across a step edge, the ordered islands are located between the height of the As-terminated GaAs step and the corresponding As-terminated GaAs terrace. This height suggests that they are indium terminated. We disregard the possibility that they are arsenic dimers, since other experiments have shown that deposition with an increased As background pressure leads to dramatically less coverage of this type of surface order. In other words, the islands become predominantly arsenic terminated.[21] The local order of the dimers appears to be a centered structure, where the neighboring [110] dimers are out of phase by 0.8 nm in the [$\bar{1}$10] direction. The dimers are spaced by 1.6 nm in the [$\bar{1}$10] direction, and 0.8 nm in the[110] direction (out of phase), indicating that the local structure is $c(4\times4)$. The dimers are infrequently observed to be ordered in a

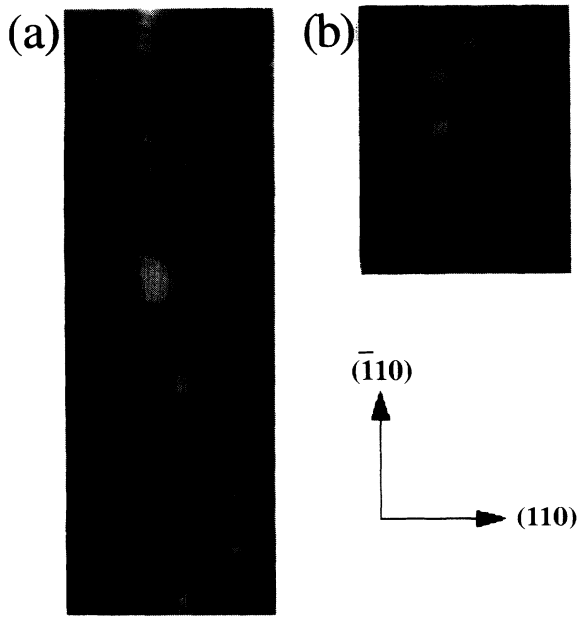

FIG. 4. Enlargements of the areas highlighted by dashed boxes in Fig. 3 are shown. An island attached to a step edge as well as small islands not associated with the step edge are shown in (a). A high-resolution zoom of an island is shown in (b). *Note* the order of the bright spots within the islands (1.6 nm apart in the [$\bar{1}$10] direction). A $c(4\times4)$ unit cell is outlined for reference in (a).

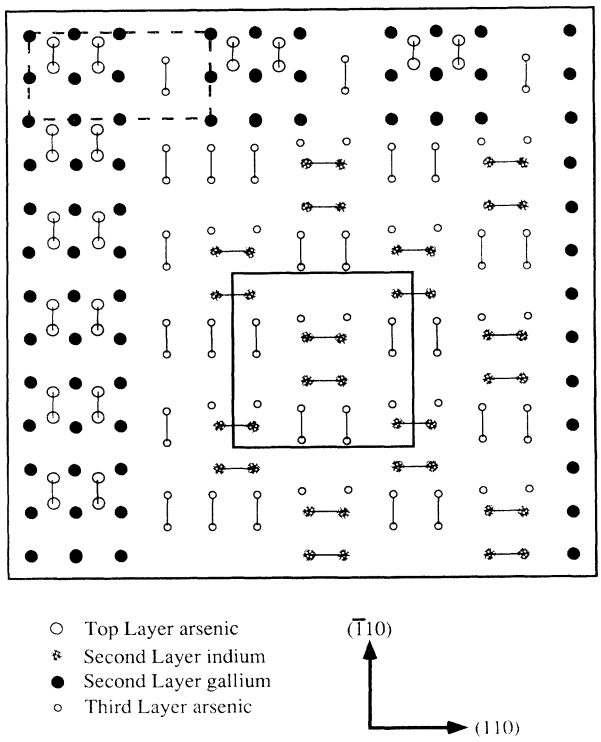

FIG. 5. A ball-and-stick model of the InAs-related $c(4\times4)$ reconstruction among unit cells of the GaAs-related (2×4) reconstruction is shown. The InAs $c(4\times4)$ unit cell is outlined with a solid line, while the GaAs (2×4) unit cell is outlined with a dashed line.

(4×4) structure, spaced 1.6 nm in the [$\bar{1}$10] direction and 1.6 nm in the [110] direction. This is in contrast to the indium-rich reconstruction generally observed for MBE-grown homoepitaxy of InAs(001), which gives a (4×2) structure.[22] The observation of a different surface reconstruction from those noted for the homoepitaxy of either material under the present conditions has been reported previously for the InAs/GaAs system.[4] In particular, a (1×3) reconstruction was observed after deposition of 0.5 ML of InAs on the GaAs(001)-c(4×4) surface at 350 °C. The most common defect observed in the local order is missing dimers of indium. Some arsenic-terminated domains on the islands are also observed, an example of which is indicated with an arrow (labeled B) in Fig. 3. These arsenic domains comprise about 13% of the islands on average, and they are ordered into a (2×n) structure.

A possible configuration of the In-terminated c(4×4) structure is shown in Fig. 5. For clarity, the model shows the InAs-related c(4×4) reconstruction along with the GaAs-(2×4) reconstruction. Although the (2×4) unit cell of GaAs shown assumes the structure proposed by Chadi,[12] the model proposed by Farrell[13] is equally viable. In the InAs-c(4×4) unit cell, outlined in Fig. 5 [cf. unit cell outlined in Fig. 4(b)], we assume that the arsenic orbitals are filled and the exposed indium orbitals are empty in order for the structure to be neutral according to electron counting rules.[23] Although the second-layer arsenic dimers are not resolved in the images, there is a decreased contrast between the indium dimers which suggests their presence (cf., Fig. 2). Although voltage-dependent images should be able to resolve the detailed structure, the samples are n doped, which causes experimental difficulties in imaging at positive sample bias.[24] Experiments with p-doped substrates, which will provide the additional insight necessary to determine the detailed structure of the unit cell, are in progress.

As shown in Fig. 3, at θ=0.35 the InAs islands are quite elongated in the [$\bar{1}$10] direction, and aspect ratios as high as 27:1 ([$\bar{1}$10]/[110]) are observed. The islands are predominantly two dimensional, although some second-layer growth is observed. A quantitative comparison of the islands formed at θ=0.15 and 0.35 is shown in Fig. 6. In Fig. 6(a) a histogram of the measured island size in the [110] direction is plotted. The mean island size was determined to be 3.9±1.1 nm at θ=0.15 and 4.0±1.0 nm at θ=0.35. Surprisingly, there has been little or no change in the island size in this direction with increasing coverage. In Fig. 6(b) a plot of the number of islands as a function of island size in the [$\bar{1}$10] direction is shown. Significant growth in the [$\bar{1}$10] direction is evi-

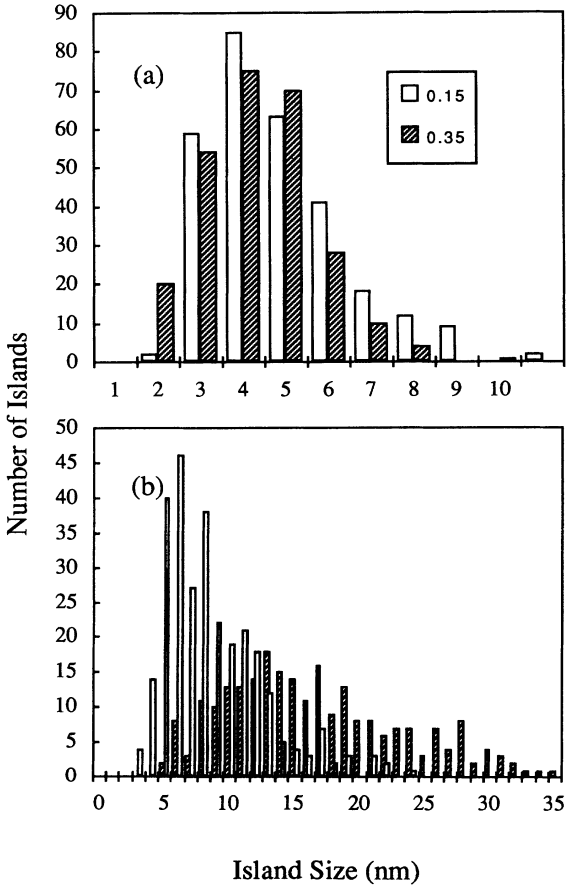

FIG. 6. A quantitative comparison of the island size in the (a) [110] direction and in the (b) [$\bar{1}$10] direction for InAs coverages of θ=0.15 and 0.35.

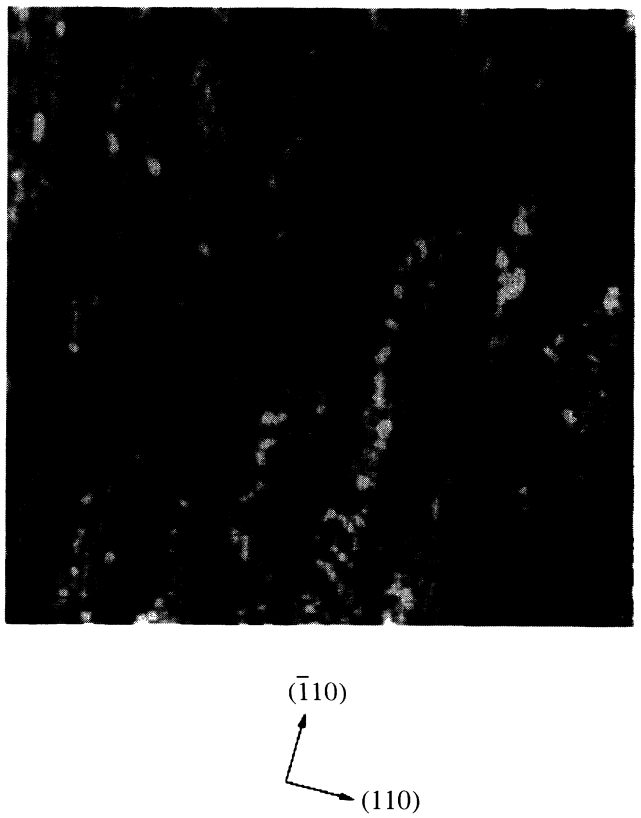

FIG. 7. A 100×100 nm^2 STM image of the 1° A-type GaAs(001)-(2×4) surface after an InAs deposition of 0.75 ML.

dent. The average island sizes measured at $\theta=0.15$ and 0.35 are 7.7 ± 3.9 and 19.3 ± 11.5 nm, respectively. The large standard deviations reflect the existence of variable island sizes in this direction. As mentioned above, the temperature is only reproducible to within $\pm10\,^{\circ}C$ for our samples during the growth. To confirm that the island anisotropy is unaffected by temperature uncertainties between different growths, we have compared the anisotropy (ratio of island sizes in the $[\bar{1}10]$ and [110] directions) of islands with *the same area* at both coverages. For $\theta=0.15$, the majority of the islands have an area ≤ 75 nm^2. Therefore, only islands with areas less than 75 nm^2 were used from the $\theta=0.35$ data set in the comparison. The distribution curves for both coverages are peaked at an aspect ratio of 3:1. From this analysis, we conclude that the difference in island-size anisotropy and the similarity in confinement of growth along the [110] direction which are observed for the two coverages are the result of kinetic or strain effects and not the result of any temperature variations.

After a deposition of 0.75 ML, the InAs islands are predominantly As terminated[25] and, thus, are no longer distinguishable from the GaAs by virtue of distinctive surface reconstructions (cf., Fig. 7). However, the step edges are well defined and the terrace width is fairly regular. As discussed in Sec. II, when 0.75 ML of InAs was deposited on the samples, the 4× RHEED pattern (measured along the $[\bar{1}10]$ direction) became a diffuse 1×. This is consistent with the image shown in Fig. 7, since no obvious periodicity in the [110] direction can be observed. Although there appears to be some 2× order in the $[\bar{1}10]$ direction, this image is not of sufficient resolution to unambiguously assign a reconstruction. The growth of InAs on GaAs at this coverage is still two dimensional, which is consistent with previous RHEED and AFM measurements which showed that the three-dimensional growth transition occurs at 1.75–2 ML.[26,27] From the images and statistical data presented here, it is clear that the growth of InAs on *A*-type GaAs(001) at this temperature proceeds by two-dimensional nucleation with the step advancing as the islands coalesce at increasing coverages.

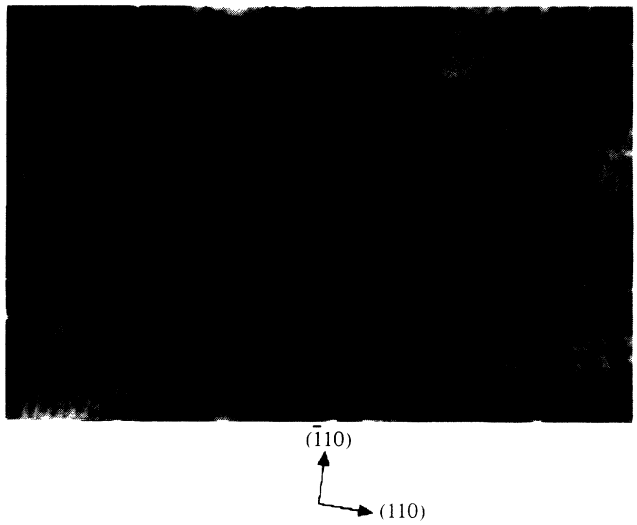

FIG. 8. A high-resolution 100×60-nm^2 STM image of 0.35 ML of InAs on the 1° *B*-type GaAs(001)-(2×4) surface. The step edges have been outlined in black. An island attached to the step edge is indicated with an arrow.

C. InAs deposition on *B*-type surfaces

Since the InAs- and GaAs-related reconstruction are clearly distinguished at $\theta=0.35$, we have chosen this coverage to investigate the growth of InAs on the *B*-type GaAs(001)-(2×4) surface. A high-resolution image of the resulting surface is shown in Fig. 8. To clarify the step edges, they have been outlined in black. As observed previously, the *B*-type surface has step edges which are irregular, and many defects are observed on the terraces such as missing rows of the (2×4) unit cell.[28] Areas of the GaAs(001)-(2×4) reconstruction are clearly visible in

TABLE I. The results of a quantitative analysis of island size and anisotropy are shown for *A*-type and *B*-type surfaces. For the *B*-type surface the islands are also analyzed with respect to the size of the terrace on which they were observed. x is the terrace width.

Sample		Island Size (nm)		
		$[\bar{1}10]$	[110]	$[\bar{1}10]/[110]$
1°-*A* type	$\theta=0.15$	7.7 ± 3.9	3.9 ± 1.5	2.1 ± 1
	$\theta=0.35$	19.3 ± 11.5	4.1 ± 1.4	4.7 ± 3
	all islands	11.5 ± 4.7	4.0 ± 1.3	3.1 ± 1.7
1°-*B* type, $\theta=0.35$	attached islands	11.3 ± 5.1	4.2 ± 1.3	2.9 ± 1.3
	$x<8$ nm	0	0	
	8 nm $<x<20$ nm	7.8 ± 2.9	3.6 ± 1.0	2.3 ± 1.2
	20 nm $<x<40$ nm	10.9 ± 4.1	4.1 ± 1.2	2.9 ± 1.5
	$x>40$ nm	12.7 ± 5.1	4.1 ± 1.3	3.4 ± 1.8

Fig. 8. As noted in Figs. 3 and 4, local (4×4) and $c(4\times4)$ ordering is observed which distinguishes the InAs from the GaAs. The local InAs structure is resolved in the terrace vacancies and at the step edges. In particular, the InAs fills in the large kinks in the GaAs step edge, which results in a smoother step edge compared to the clean GaAs surface. Compared to the *A*-type surface, there is more growth at step edges on this surface. This is not surprising considering the anisotropy of the islands observed on the *A*-type surface, which suggested that the reactivity of the anion-terminated step edge is greater than the reactivity of the cation-terminated step edge.[18] Anisotropic diffusion may also play a role; however, the diffusion length of In at this temperature is expected to be large in both directions.[1,2] There are areas of the step edges, however, which have not reacted with InAs, indicating that even on this surface the *absorption* probability of the step edge is not unity.

Generally, on the *B*-type surface there are no InAs islands observed on GaAs terraces which are less than 8 nm wide. Here islands attached to the step edge are defined as structures which are enclosed by kinks at least four unit cells in extent. When the terrace width increases (> 8 nm), islanding is observed. We also observe that 30% of the islands grow out of the step edge. An attached island is indicated with an arrow in Fig. 8. All islands have the same characteristic width distribution in the [110] direction that was observed on the *A*-type surface, whereas the size of the islands in the $[\bar{1}10]$ direction was found to be dependent on the corresponding terrace width. The InAs islands were never observed to create a double step. The results of a quantitative analysis of the islands observed on *B*-type surfaces are presented in Table I. For comparison, data from the *A*-type step are also included. In Sec. IV, we will discuss islands on the *B*-type surface first, and then compare the results to islands on the *A*-type surface.

IV. DISCUSSION

The InAs islands attached at the step edge and the islands found on the terrace are not statistically different. The terrace width for the *B*-type surface, however, plays an important role in determining the growth in the $[\bar{1}10]$ direction. To quantify the relation between terrace width and island shape, we have separately analyzed the islands according to the terrace size. As shown in Table I, the anisotropy of the islands for the *B*-type surface increases with increasing terrace width. This indicates that the width of the terrace (barrier at the step edge) is limiting growth in the $[\bar{1}10]$ direction. However, the size of the islands in the [110] direction remains constant (within ±1 nm) irrespective of the terrace width. Furthermore, it is the same size that is observed on the *A*-type step (cf., Table I).

The occurrence of a preferred width of islands in the [110] direction, independent of the surface misorientation or the coverage ($\theta < 0.75$ ML), could be due to chemical differences of the steps, to anisotropic diffusion, or to the influence of strain. The edge of an InAs island along the $[\bar{1}10]$ direction is terminated with indium and can be considered to be an *A*-type step edge. Likewise, an InAs island edge along the [110] direction is terminated with arsenic and can be considered to be a *B*-type step edge. For equilibrium growth conditions, we expect the anisotropy of the islands to be dictated by the energetics at the step edges.[29] Hence the observed anisotropy of the InAs islands and the increased InAs growth at the *B*-type step compared to the *A*-type step indicate that the arsenic-terminated step edge is more reactive during the growth of InAs. However, the reaction anisotropy of the step edge does not account for the InAs islands remaining constant at 4 nm along the [110] direction regardless of coverage, since the anisotropy dictated by the step energetics will not change as a function of coverage. The anisotropy of the InAs islands also suggests that there is increased diffusion in the $[\bar{1}10]$ direction which would result in slower growth of the *A*-type island edge with increasing coverage. Nevertheless, the observed diffusion anisotropy cannot account for the preferred InAs island size observed in the [110] direction. On the *B*-type surface, diffusion along $[\bar{1}10]$ is reduced because of the presence of step edges. For large terraces (> 8 nm), this would lead to more growth in the [110] direction compared to the *A*-type surface. This is clearly not observed (cf., Table I). The influence of strain in the InAs islands could explain the constant island width in the [110] direction irrespective of coverage ($\theta < 0.75$) and surface misorientation. With increasing island width, the strain increases until the attachment of additional atoms is no longer energetically favorable and no further island growth takes place.

We conjecture that the edges of the islands along the $[\bar{1}10]$ direction relax to accommodate the strain and that 4±1 nm (in the [110] direction) is the preferred size for this relaxation. Support for the existence of a preferred island size for submonolayer coverages comes from *in situ* RHEED measurements.[30] It was observed that for $In_xGa_{1-x}As$ ($x=0.49$) on nominally flat GaAs(001) (mismatch ~4%), the lattice constant oscillates within a monolayer of coverage, with maximum relaxation ($\Delta a_{\parallel}/a_{\parallel}^{GaAs}$ of 0.3%) occurring at $\theta=0.5$ ML. Moreover, from a one-dimensional model of the surface, it was determined that this elastic relaxation corresponds to islands with a lateral extent of 4.4 nm covering half of the surface. The islands we observe have, on average, a lateral extent in the [110] direction of 4 nm. There is good agreement between predicted and measured values even though the strain of $In_xGa_{1-x}As$ (4%) is less than InAs (7%) on the GaAs(001) surface. Moreover, the InAs islands are not isotropic. There is considerable growth and nonuniformity of the islands in the $[\bar{1}10]$ direction. The fact that growth seems not to be limited in the $[\bar{1}10]$ direction indicates that most of the strain is accommodated by elastic deformation along the [110] direction. In addition, the $c(4\times4)$ reconstruction of the InAs may be reducing strain in this direction. Calculations demonstrating the effect of strain on island growth which include the surface reconstruction and the anisotropy of surface diffusion and step-edge reactivities would be useful for a more detailed understanding of strained growth

in the present material system.

It is surprising that we do not observe predominant step-edge nucleation of InAs on either A- or B-type surfaces. This could be a consequence of the growth temperature, i.e., at 450 °C indium may not be able to diffuse to the step edge before nucleating with another indium atom or attaching to an existing island. However, as stated previously, the anisotropy of the islands observed on the A-type surface, with some islands as long as 70 nm, suggest that we are at a temperature where the indium atoms should be easily able to diffuse to the B-type step. Recent theoretical work by Ratsch and Zangwill[31] has suggested that growth at the step edge is more strained than growth on the terrace. In particular, these authors suggested that strain reduces the energy barrier to adatom detachment more for large islands than for small islands, with the barriers most reduced at the step edge. They concluded that significantly strained systems would be driven away from step-flow growth into growth characterized predominantly by the coalescing of islands. We believe that this is the growth mode we have observed for InAs deposited on GaAs(001), and suggest that the lack of step-edge nucleation is a result of strain.

V. CONCLUSIONS

In summary, we have studied MBE-grown vicinal GaAs(001)-(2×4) surfaces after submonolayer deposition of InAs at 450 °C. The InAs forms islands that are locally ordered into a (4×4) or a $c(4\times4)$ indium-terminated reconstruction, which easily distinguishes them from the (2×4) GaAs surface. From the images and statistical data derived therefrom, it is clear that the growth of InAs on A-type GaAs at this temperature preceeds by two-dimensional nucleation, with the step advancing as the islands coalesce at increasing coverages. On B-type surfaces, on the other hand, InAs nucleates predominantly, but not exclusively, at the step edges and in the vacancies on the terraces. Island growth is observed only on terraces larger than 8 nm, with the anisotropy of the islands depending on the corresponding terrace width. Regardless of coverage or surface misorientation, InAs islands are observed to have a preferred width of 4 nm in the [110] direction. We conjecture that strain effects are limiting the island size in the [110] direction.

ACKNOWLEDGMENTS

We gratefully acknowledge financial support by QUEST, NSF Science and Technology Center for Quantized Electronic Structures (Grant No. DMR 91-20007), AFOSR Grant No. (F49620-J-0214), a MICRO-SBRC grant, and the W. M. Keck Foundation. One of us (V.B.H.) gratefully acknowledges support from Rockwell. We would like to thank W. Widdra for helpful discussions.

*Present address: Universitat München, Sektion Physik, Geschwister-Scholl-Platz 1, 80539 München, Germany.

[1]D. Leonard, M. Krishnamurthy, C. M. Reaves, S. P. Denbarars, and P. M. Petroff, Appl. Phys. Lett. **63**, 3203 (1993).

[2]O. Brandt, L. Tapfer, K. Ploog, R. Bierwolf, M. Hohenstein, F. Phillipp, H. Lage, and A. Heberle, Phys. Rev. B **44**, 8043 (1991).

[3]A. Lorke, T. Noda, Y. Nagmune, Y. Nakamura, H. Sugawara, and H. Sakaki, in *Proceedings of the 21st International Conference on the Physics of Semiconductors, China, 1992* (World Scientific, Singapore, 1994), p. 1258.

[4]S. M. Scholz, A. B. Muller, W. Richter, D. R. T. Zahn, D. I. Westwood, D. A. Woolf, and R. H. Williams, J. Vac. Sci. Technol. B **10**, 1710 (1992).

[5]K. H. Ploog and O. Brandt, Semicond. Sci. Technol. **8**, S229 (1993).

[6]The TSL was grown to improve the periodicity of the surface. See, for example, K. Pond, A. Lorke, J. Ibbetson, V. Bressler-Hill, R. Maboudian, W. H. Weinberg, A. C. Gossard, and P. M. Petroff (unpublished).

[7]J. M. Moison, C. Guille, M. Van Rompay, F. Barthe, F. Houzay, and M. Bensoussan, Phys. Rev. B **39**, 1772 (1989); A. Lorke, M. Krishnamurthy, and P. M. Petroff, in *Common Themes and Mechanisms of Epitaxial Growth* edited by P. Fuoss, J. Tsao, D. W. Kisker, A. Zangwill, and T. F. Kuech, MRS Symposia Proceedings No. 312 (Materials Research Society, Pittsburgh, 1993), p. 65.

[8]It has been shown that the MBE growth of GaAs on B-type GaAs(001), after layer thicknesses greater than 0.2 μm, results in no obvious step bunching at the surface. See I. G. Tanaka, S. Ohkouchi, and A. Hashimoto, Jpn. J. Appl. Phys. **31**, 2216 (1992).

[9]E. Tournie, O. Brandt, C. Giannini, K. H. Ploog, and M. Mohenstein, J. Cryst. Growth **127**, 765 (1993).

[10]X.-S. Wang, C. Huang, V. Bressler-Hill, R. Maboudian, and W. H. Weinberg, J. Vac. Sci. Technol. A **11**, 2860 (1993).

[11]V. Bressler-Hill, M. Wassermeier, K. Pond, R. Maboudian, G. A. D. Briggs, P. M. Petroff, and W. H. Weinberg, J. Vac. Sci. Technol. B **10**, 1881 (1992); R. Maboudian, V. Bressler-Hill, and W. H. Weinberg, Phys. Rev. Lett. **70**, 3172 (1993).

[12]D. J. Chadi, J. Vac. Sci. Technol. A **5**, 843 (1987).

[13]H. H. Farrell, J. P. Harbison, and D. L. Peterson, J. Vac. Sci. Technol. B **5**, 1482 (1987).

[14]R. Maboudian, V. Bressler-Hill, K. Pond, X. S. Wang, P. M. Petroff, and W. H. Weinberg, Surf. Sci. Lett. **302**, L269 (1994).

[15]J. Sudijono, M. D. Johnson, C. W. Snyder, M. B. Elowitz, and B. G. Orr, Phys. Rev. Lett. **69**, 2811 (1992).

[16]T. Ide, A. Yamashita, and T. Mizutani, Phys. Rev. B **46**, 2675 (1992).

[17]E. J. Heller and M. G. Lagally, Appl. Phys. Lett. **60**, 2675 (1992).

[18]V. Bressler-Hill, R. Maboudian, M. Wassermeier, X.-S. Wang, K. Pond, P. M. Petroff, and W. H. Weinberg, Surf. Sci. **287/288**, 514 (1993).

[19]Y. Horikoshi, H. Yamaguchi, F. Briores, and M. Kawashima, J. Cryst. Growth **105**, 326 (1990).

[20]K. Shiraishi, Appl. Phys. Lett. **60**, 1363 (1992).

[21]V. Bressler-Hill, S. Varma, A. Lorke, P. M. Petroff, and W. H. Weinberg (unpublished).

[22]H. Yamaguchi and Horikoshi, Phys. Rev. B **48**, 2807 (1993).

[23]W. A. Harrison, J. Vac. Sci. Technol. **16**, 1492 (1979).

[24]R. Maboudian, K. Pond, V. Bressler-Hill, M. Wassermeier, P. M. Petroff, G. A. D. Briggs, and W. H. Weinberg, Surf. Sci.

Lett. **275**, L662 (1992).
[25]The sample was grown with an increased As-background pressure.
[26]J. Moison, F. Houzay, F. Barthe, and L. Leprince, Appl. Phys. Lett. (to be published).
[27]D. Leonard and K. Pond (private communication).
[28]M. D. Pashley, K. W. Haberern, and J. M. Gaines, Appl. Phys. Lett. **58**, 406 (1991).
[29]M. G. Lagally, Y.-W. Mo, R. Kariotis, B. S. Swartzentruber, and M. B. Webb, in *Kinetics of Ordering and Growth at Surfaces,* edited by M. G. Lagally (Plenum, New York, 1990), p. 145.
[30]J. Massies and N. Grandjean, Phys. Rev. Lett. **71**, 1411 (1993).
[31]C. Ratsch and A. Zangwill, Appl. Phys. Lett. **63**, 2348 (1993).

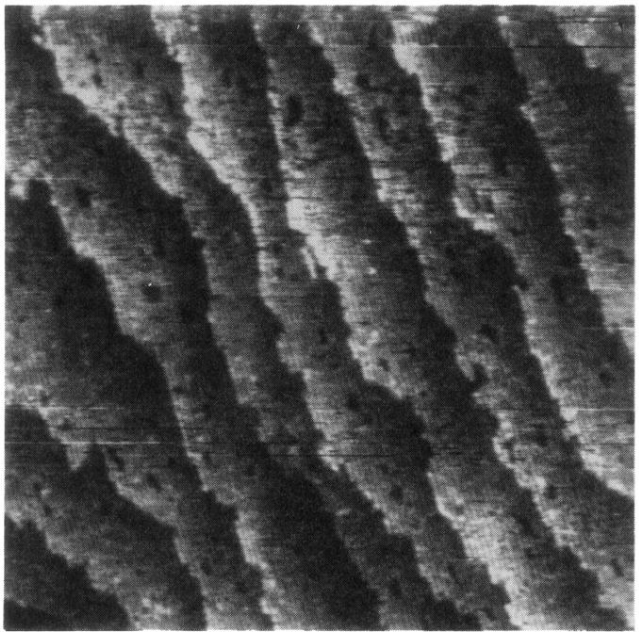

FIG. 1. A 200×200 nm^2 STM image of a clean 1° *A*-type GaAs(001)-(2×4) surface.

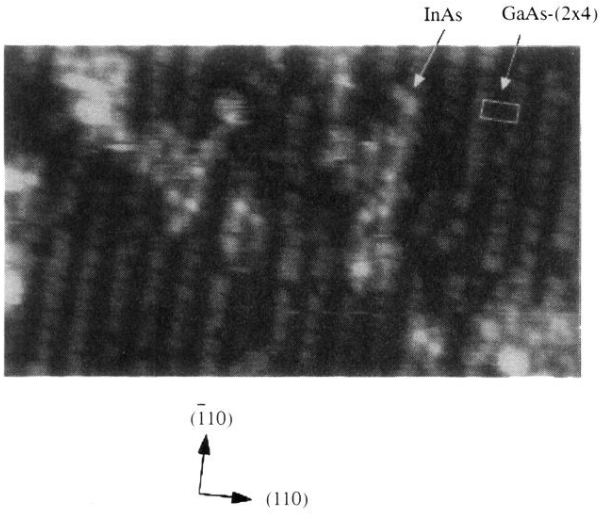

FIG. 2. A high-resolution STM image of the 1° *A*-type GaAs(001)-(2×4) surface after deposition of 0.15 ML of InAs. Note the clear resolution of the GaAs-related (2×4) unit cell. An InAs island is indicated with an arrow. The size of the image is 30×15 nm^2.

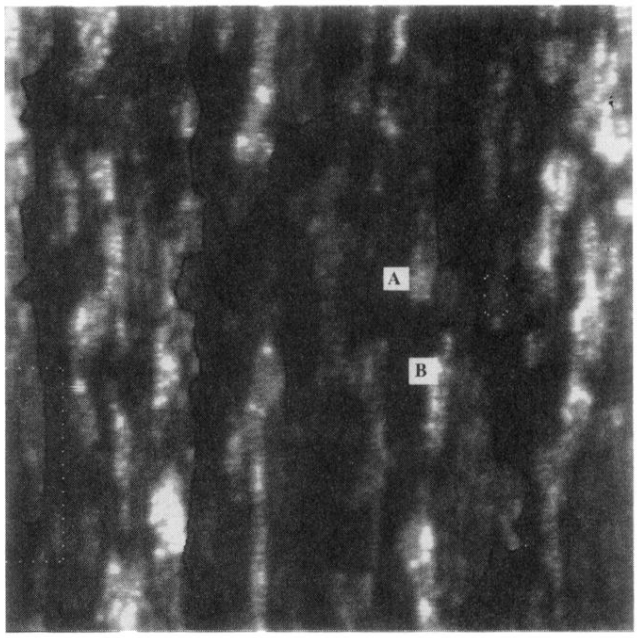

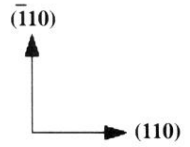

FIG. 3. A 100×100-nm^2 STM image of the 1° A-type GaAs(001)-(2×4) surface with an InAs coverage of $\theta=0.35$. For clarification, the step edges have been outlined in black. Note the anisotropy of the InAs islands. Some islands exhibit separate domains of indium and arsenic termination. An In-terminated domain (A) and an As-terminated domain (B) are indicated with arrows. The areas that are highlighted with the dashed line are shown in Fig. 4.

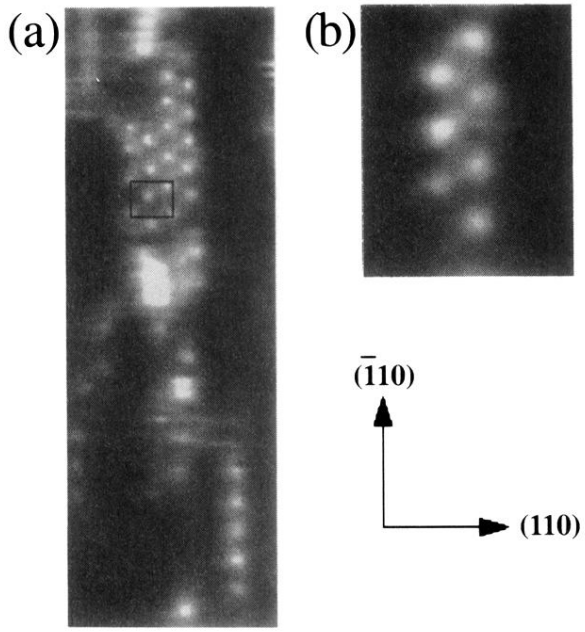

FIG. 4. Enlargements of the areas highlighted by dashed boxes in Fig. 3 are shown. An island attached to a step edge as well as small islands not associated with the step edge are shown in (a). A high-resolution zoom of an island is shown in (b). Note the order of the bright spots within the islands (1.6 nm apart in the $[\bar{1}10]$ direction). A $c(4\times4)$ unit cell is outlined for reference in (a).

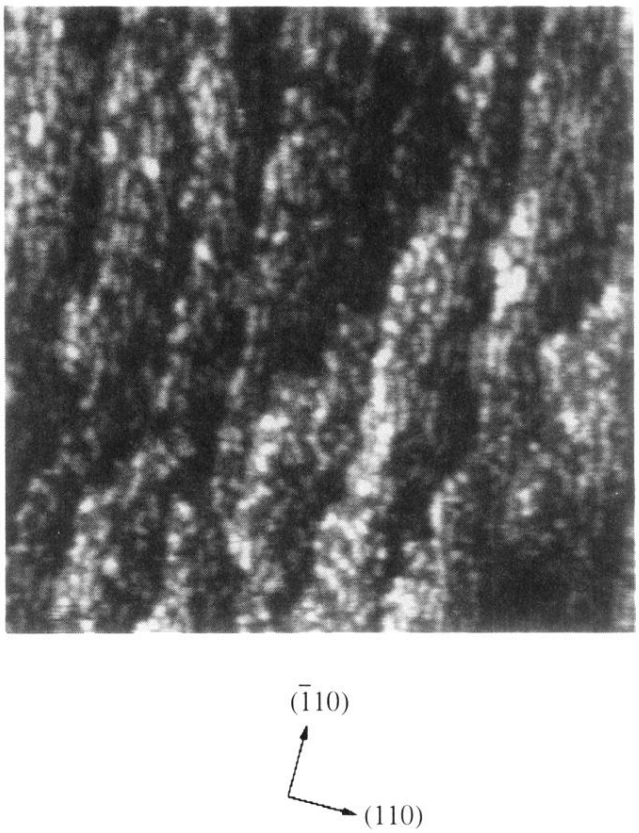

FIG. 7. A 100×100 nm^2 STM image of the 1° *A*-type GaAs(001)-(2×4) surface after an InAs deposition of 0.75 ML.

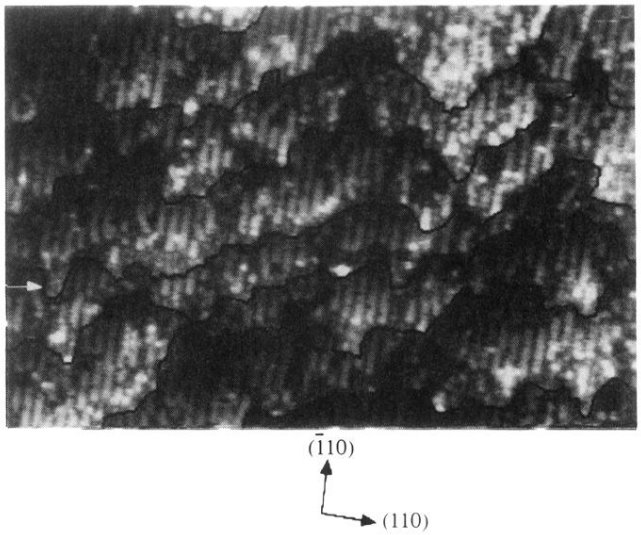

FIG. 8. A high-resolution 100×60-nm^2 STM image of 0.35 ML of InAs on the 1° *B*-type GaAs(001)-(2×4) surface. The step edges have been outlined in black. An island attached to the step edge is indicated with an arrow.